Bioreduction

DOI: 10.1002/anie.201207070

Tracking the Bioreduction of Disulfide-Containing Cationic Dendrimers**

*Lorine Brülisauer, Nadia Kathriner, Mark Prenrecaj, Marc A. Gauthier, and Jean-Christophe Leroux**

Responsiveness to endogenous reduction (that is, bioreduction) is increasingly used to improve the properties of biomaterials and drug delivery systems.[1] Successful exploitation of this phenomenon relies on the precisely timed, predictable, and location-specific scrambling of a disulfide bond incorporated into the system. While the properties of the disulfide bond can be controlled through steric hindrance, the electrostatic microenvironment, and strain,[2] only a limited and often qualitative picture of the location/extent of bioreduction in the presence of cells is available.[3] Such knowledge is indispensable for enhancing the efficacy of these systems and for correctly interpreting experimental results.

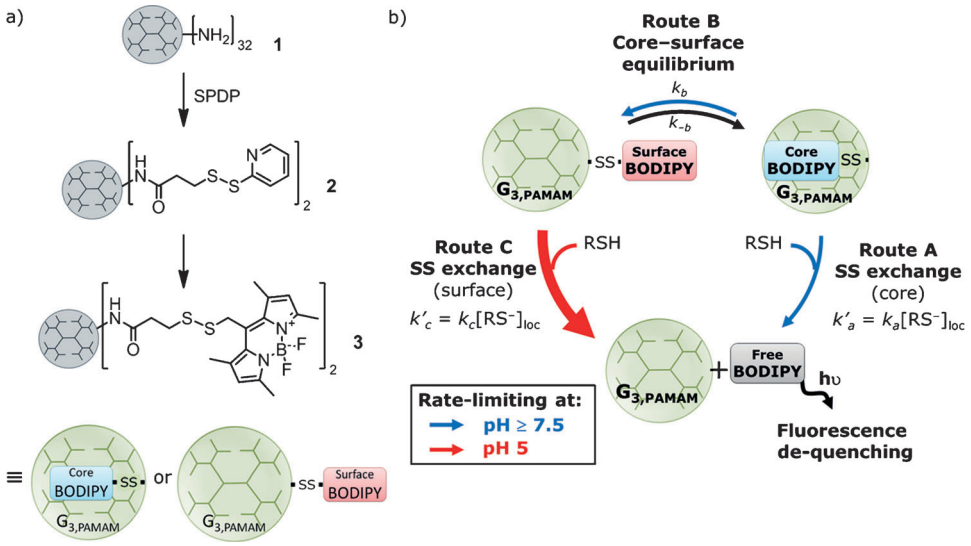

Figure 1. a) Synthesis of a dual-responsive redox-sensitive probe **3** from a third-generation (G_3) PAMAM dendrimer (**1**). b) The hydrophobic BODIPY fluorophores partition between the surface and the core of the dendrimer, which provides models for exposed and buried disulfide bonds, respectively.

We have recently shown a quantitative relationship between the net positive charge of the microenvironment around disulfide bonds and an acceleration of thiol–disulfide exchange owing to electrostatic interactions with the reducing agent.[2b] Based on this phenomenon, the high positive charge of cationic gene delivery systems should make their bioreducible analogues highly susceptible to disulfide exchange. Disulfides have notably been used in gene delivery systems for attaching targeting/shielding moieties, stabilizing the complexes, and for promoting biodegradation/release of cargo.[1c,4] Indeed, while most of these systems are designed for intracellular bioreduction, some studies have reported that this can occur extracellularly,[3d,e] in accordance with our hypothesis above. Early bioreduction can have a dramatic effect on the interpretation of data and influence the expected mechanism of toxicity, uptake pathway, and ultimate efficacy.[5] Overall, the actual behavior of disulfide bonds within this class of system has received little attention.

This study quantitatively investigates the bioreduction of a dynamic disulfide-containing probe (**3** in Figure 1a) based on cationic poly(amido amine) dendrimers (PAMAM; **1**), which are widely used carriers for nucleic acid delivery. PAMAM is ideally suited for mechanistic studies owing to their homogeneity of size and structure, which allows for quantitative analysis of the influence of electrostatic interactions on disulfide exchange.[2b] In this work, a third-generation PAMAM (**1**) was selected because it is relatively well-tolerated by cells, does not induce membrane hole formation,[6] and should provoke less osmotic swelling (versus higher generation PAMAM), which combined should enable the study of bioreduction early in the trafficking process without interference of disulfide exchange in the cytoplasm. About two boron dipyrromethene (BODIPY) fluorophores were grafted to **1** by a *N*-succinimidyl 3-(2-pyridyldithio)-propionate linker that contains a disulfide bond (**3**). Compound **3** has the particularity that BODIPY dynamically partitions between surface and core states (Figure 1b), which

[*] L. Brülisauer, N. Kathriner, M. Prenrecaj, Dr. M. A. Gauthier, Prof. Dr. J.-C. Leroux
Swiss Federal Institute of Technology Zurich (ETHZ)
Department of Chemistry and Applied Biosciences
Institute of Pharmaceutical Sciences
Wolfgang-Pauli-Strasse 10, 8093 Zurich (Switzerland)
E-mail: jleroux@ethz.ch

[**] L. B. acknowledges the Scholarship Fund of the Swiss Chemical Industry (2-70882-08). The Light Microscopy Center (ETHZ) and Alois Renn are thanked for experimental support. Ari Helenius kindly provided RFP-Rab5 plasmids.

Supporting information for this article is available on the WWW under http://dx.doi.org/10.1002/anie.201207070.

allows simultaneously probing of the bioreduction of solvent-exposed (for tethering ligands) and buried disulfide bonds (for biodegradation of polycations). This dynamic partitioning arises from pH-dependent equilibration of the hydrophobic BODIPY between the hydrophilic and charged environment at the surface of **3**, and its hydrophobic core, which is mostly deprotonated at neutral pH. Such a pH-dependent conformational change of **3** was suggested by ^{1}H NMR spectroscopy and by fluorescence lifetime measurements (Supporting Information, Figures S5 and S6). Resonant-energy transfer between BODIPY dyes in intact **3** suppressed fluorescence, whilst exchange/reduction of even a single disulfide bond produced a high (ca. 10-fold) increase of fluorescence intensity (Figure 2), which was used for quantifying disulfide shuffling. A quantitative analysis of the influence of electrostatic interactions on disulfide exchange of **3** was performed to determine the rate constants k_{a-c} in Figure 1 b (Supporting Information).

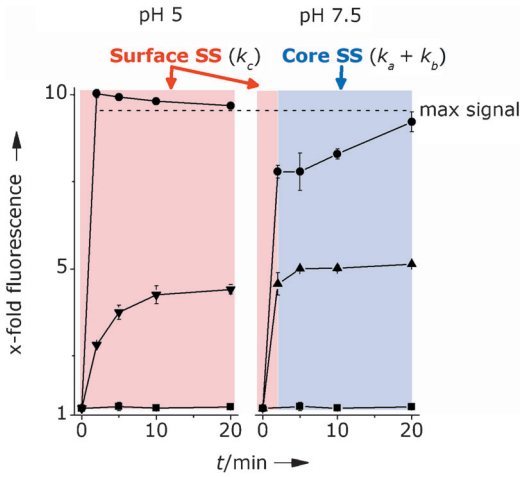

Figure 2. Surface-exposed fluorophores of **3** (500 nM) are rapidly exchanged by route C (red areas), whilst the core fluorophores (blue area) are exchanged substantially more slowly by the rate-determining routes A and B. ● 90 mM GSH, ▲ 1 mM GSH, ▼ 10 μM GSH, ■ no reducing agent. Data presented as mean ± S.D. ($n = 3$).

At neutral pH, BODIPY partitioned more or less equally between both surface and core states, as seen by a very rapid 50–60 % dequenching before the 2 min time point in the presence of reducing agent, which was attributed to exchange of surface disulfide bonds (1 mM glutathione (GSH) in Figure 2; Supporting Information, Figures S7 and S9). The GSH concentrations used to analyze the dequenching kinetics correlated to the amount found in the body (1–11 mM GSH in cytoplasm and about 10 μM in the extracellular space).[1c] The determined rate constant for exchange of surface disulfides ($k_c \approx 2.5 \times 10^5$ L mol^{-1} h^{-1}) was comparable to other disulfides with similar steric hindrance, which lends credibility to the model.[2b] Following this rapid dequenching, fluorescence recovery continued at a slower rate owing to exchange of core disulfides ($k_a = 0.30$ L mol^{-1} h^{-1}) and to transfer of BODIPY from the core to the surface ($k_b = 0.35$ h^{-1}). Owing to the relatively low values for k_a and k_b, this process is best observed at high GSH concentrations (90 mM), but was also observed at lower GSH concentrations (1 mM GSH; Figure 2 and Supporting Information, Figure S9). Note that dequenching continues beyond the 20 min time point for all kinetic curves in this study where the maximum signal was not seen, the exception being 10 μM GSH where plateaus were observed owing to oxidation of the weak redox buffer. Careful analysis of this second part of the dequenching curve under a variety of conditions permitted the determination of k_a and k_b (Supporting Information).

To confirm that partitioning between surface and core states was responsible for this dual disulfide bond behavior, dequenching of **3** was analyzed in acidic medium, in which the core amino groups are protonated, thus forcing BODIPY to the surface state. This was confirmed by the rapid and now complete dequenching of **3** before the first time point (90 mM GSH, pH 5; Figure 2 and Supporting Information, Figure S8). Owing to the polycationic nature of **3**, which induces a local accumulation of GSH, disulfide exchange of surface-exposed disulfides was rapid, even with as little as 10 μM GSH at pH 5 (40 % in less than 20 min). Using a neutral reducing agent (cysteamine; Supporting Information, Figures S7 and S8) with no electrostatic accumulation resulted in slower disulfide exchange kinetics of **3** at pH 5, which confirmed the accumulation effect of GSH. These results underline that both exposed and buried disulfide bonds in polycations are highly susceptible to bioreduction owing to electrostatic interactions with charged reducing agents and points to the necessity of analyzing bioreduction in the early stages of cellular trafficking.

Four human cancer cell lines were selected for analysis. Compound **3** was incubated with colorectal, prostate, lung, and cervical adenocarcinoma cells (Caco-2, PC3, A549, and HeLa) and total (intra and extracellular) fluorescence was quantified with time. As seen in Figure 3 a, bioreduction was linear with time over 2 h rather than the expected dual responsiveness observed in Figure 2 coming from the sequential bioreduction of surface and core disulfide bonds. This lack of distinction between the two exposed and buried disulfide states suggests that species other than small-molecule reduc-

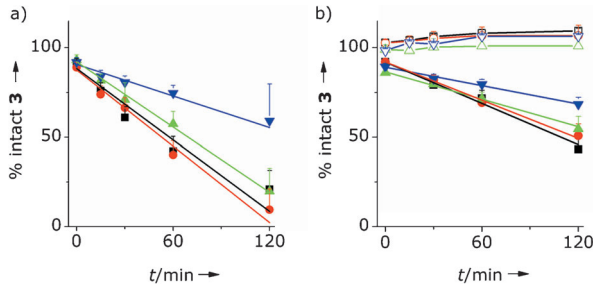

Figure 3. Bioreduction of **3** (150 nM) by four different cell lines (■ A549, ● HeLa, ▲ PC3, ▼ Caco-2) either alone (a) or in the presence of DTNB (5 mM) (b). In (b), the open symbols correspond to co-incubation with DTNB to continuously oxidize thiols released by the cell, and closed symbols correspond to a pulse-wash application of DTNB to uniquely oxidize cell-surface thiols at time zero. Data are plotted as % intact **3** over time with a 10-fold increase in fluorescence used as complete dequenching. Results are expressed as mean ± S.D. ($n = 9$).

ing agents were involved in bioreduction. These could include cell-surface oxido reductases (for example, protein disulfide isomerase, PDI)[1a,c] and/or chaperones (also PDI),[7] as the latter may exert a "protein refolding-like" activity on **3** that accelerates molecular dynamics of the core to surface equilibrium. Figure 3a confirms the sensitivity of **3** to bioreduction, which was complete within 2 h for all cells except Caco-2, independently of whether the disulfides were solvent-exposed or not. Co-incubation of **3** with 5,5′-dithiobis(2-nitrobenzoic acid) (DTNB, a membrane-impermeable thiol oxidant) and cells completely suppressed bioreduction, indicating that fluorescence dequenching was due uniquely to bioreduction (Figure 3b). A thiol-insensitive analogue of **3** (**5**; Supporting Information) also showed no fluorescence increase in the presence of cells (Supporting Information, Figure S15).

To better analyze the extracellular agents involved in bioreduction, the cell surface was pre-oxidized by pulse-wash treatment with DTNB. Interestingly, rather than producing a lag in the bioreduction of **3** (during which oxido reductases are regenerated by secreted thiols), a decreased rate of exchange of the probe by precisely a factor of two was observed for all cell lines (Figure 3b; Supporting Information, Table S3). This fact points to a common phenomenon, which could implicate inactivation of one of the two active sites of PDI owing to conformational changes or (hetero)oligomerization.[8] It should be noted that during the timeframe of the experiment, the secretion of fresh thiol oxido reductases was expected to be minimal.[9] In addition, the observed rates of dequenching of **3** (that is, the slope; Supporting Information, Table S3) correlated reasonably well with the concentration of secreted thiols (not cell-surface associated; Supporting Information, Table S4), despite the fact that four different cell lines were examined (Supporting Information, Figure S16). This result indicates that secreted thiols (likely GSH) probably act as co-factors for oxido reductases without direct involvement in bioreduction, as otherwise a dual-responsiveness would be observed as in Figure 2. Cells treated with inhibitors of endocytosis (Supporting Information, Figure S17) showed a comparable proportionality (Supporting Information, Figures S16 and S18), supporting the hypothesis that bioreduction of **3** occurs entirely extracellularly. These data suggest that the cell surface (most likely proteins) is strongly involved in bioreduction.

To analyze the influence of plasmid DNA on the accessibility of the disulfide bonds within **3**, a series of complexes with N/P (nitrogen to phosphate) molar ratios from 10–1.5 were prepared. For consistency, surface and core continue to refer to the state of BODIPY within **3** and not to their location within the complex of **3** with pDNA. In comparison to **3** alone, disulfide exchange of both surface (red area) and core (blue area) disulfides with GSH (no cells) was slowed down with increasing pDNA content (Figure 4a). While this highlights the expected increased steric hindrance resulting from the presence of pDNA, it is interesting to note that it was still possible to distinguish a dual-behavior resulting from exchange of BODIPY in surface and core states, although the distinction between the two is less obvious for N/P 1.5. At this N/P ratio, the complexes were the most

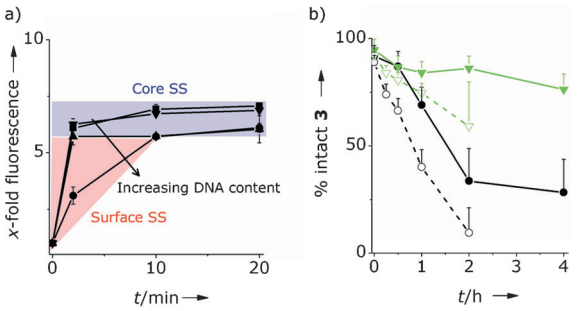

Figure 4. a) Fluorescence dequenching of **3** (500 nM) at pH 7.4 in the presence of 1 mM GSH (■) and variable amounts of pDNA to yield N/P molar ratios of 10 (▼), 5 (▲), and 1.5 (●). Disulfide exchange is slowed with increasing amounts of pDNA. N/P 10: no difference; N/P 5: Core disulfide exchange slowed; N/P 1.5: Both surface and core disulfide exchange slowed and less distinguishable from one another. b) Stability of **3** (150 nM, -----) and **3**-pDNA (N/P 1.5, ——) in the presence of HeLa (●,○) and Caco-2 (▼,▽) cells. Results are expressed as mean ± S.D. ($n=3$).

compact and uniform (Supporting Information, Figure S19) and the effect of pDNA on disulfide exchange was maximal. This prompted their analysis in the presence of HeLa and Caco-2 cells (the most and least reducing cell lines from above; Figure 4b). Consistent with above, the nanoparticles showed a reduced rate of bioreduction versus **3** alone. However, a distinction between disulfides in surface and core states then became apparent for the **3**-pDNA complex with HeLa cells (not observed for Caco-2 cells because of insufficient bioreduction). This result indicates that the steric barrier imparted by pDNA may mitigate the effect of cell-surface proteins suspected in facilitating the bioreduction of core disulfide bonds above. This result points to extracellular bioreduction of systems shielded with macromolecules (for example, poly(ethylene glycol))[3d] as resulting from small molecule reductants, rather than cell-surface proteins. As the concentration of these reductants is generally low, shielding may provide a means for (at least) partially stabilizing disulfide bonds from these reactive species.

As incomplete bioreduction was observed for Caco-2 cells, intracellular processing was examined. Figure 5a shows a slight increase in fluorescence of cell-associated **3** over 2 h, which could result from bioreduction in the intra and/or extracellular space. After 2 h, addition of GSH monoethylester (GSHOEt, a membrane-permeable reductant) led to a large increase in fluorescence intensity, confirming incomplete bioreduction of **3**, in agreement with Figure 3a. This experiment, however, cannot distinguish extra from intracellular bioreduction. To analyze if the endocytic/lysosomal compartments are implicated in disulfide exchange, cell-associated **3** was co-incubated with chloroquine (150 μM). Chloroquine is an endosomolytic agent that should facilitate the rupture of endosomes/lysosomes and promote transit of any internalized **3** to the cytosol. Co-incubation with chloroquine led to a substantially stronger recovery of fluorescence (Figure 5b) than **3** alone owing to exposure of the endocytosed probe to cytoplasmic reducing agents. This result indicated that **3** remained largely intact within the endocytic compartments. The limited disulfide exchange observed in

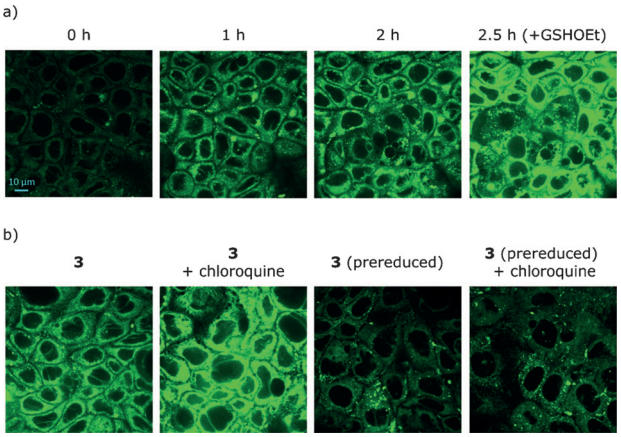

Figure 5. a) Representative confocal microscopy images of Caco-2 cells incubated with cell-associated **3** over 2.5 h at 37 °C. After the 2 h time point, GSHOEt (2 mM) was added to promote disulfide exchange in the intra and extracellular space. b) Representative confocal microscopy images of Caco-2 cells with cell-surface associated **3** or prereduced **3**. Cells were either incubated in the absence or presence of chloroquine (150 µM) for 3 h at 37 °C. Chloroquine led to a strong increase of fluorescence for **3**, but not for prereduced **3**. These results suggest that disulfide exchange is inefficient in the endosomal/lysosomal processing of **3** in Caco-2 cells, but can occur in the cytoplasm, where the concentration of reducing agents is higher. λ_{ex}: 488 nm, λ_{em} filter: 520/35.

these organelles suggests the presence of low concentrations of reducing agent, as acidity should promote a shift of all BODIPY to the surface state, where the disulfide bond becomes highly sensitive to bioreduction (Figures 1b and 2). These results indicate that efficient bioreduction in the endosomes, while sometimes reported,[1c,3c,h] is not a universal phenomenon and should be verified for each new system and its corresponding target cell line.

In summary, the kinetic analysis of **3** confirmed that the strong positive charge of bioreducible gene delivery polymers makes them very sensitive to disulfide exchange, and that this occurs to a large extent (if not entirely) in the extracellular space. The dynamic nature of **3** further suggested the implication of cell-surface oxido reductases and/or chaperones in the bioreduction process, which facilitate the bioreduction of buried disulfide bonds. This study also highlights cell line specific differences, which stresses the need for analyzing the reducing potential of cell lines of interest prior or concurrent with vector design. Overall, these findings offer new insight for explaining the reduced cytotoxicity and improved transfection efficacy that bioreduction imparts to gene delivery systems. For instance, as the cytotoxicity of polycationic gene delivery polymers scales with concentration, increasing molecular weight, and charge density,[5a–c] early bioreduction in systems containing disulfide bonds might expose the cells to lower molecular weight (and/or potentially less branched) polycations with decreased cytotoxicity. Furthermore, rapid formation of mixed disulfides with the cell surface[5d,10] may lead to enhanced endocytosis by an anchoring effect. Such knowledge will be indispensible for the future design and optimization of bioreducible gene delivery systems.

Received: August 31, 2012
Published online: November 5, 2012

Keywords: bioreducibility · dendrimers · disulfide · drug delivery · poly(amidoamine)

[1] a) G. Saito, J. A. Swanson, K.-D. Lee, *Adv. Drug Delivery Rev.* **2003**, *55*, 199–215; b) A. M. Wu, P. D. Senter, *Nat. Biotechnol.* **2005**, *23*, 1137–1146; c) S. Bauhuber, C. Hozsa, M. Breunig, A. Göpferich, *Adv. Mater.* **2009**, *21*, 3286–3306; d) H. Fang, K. Zhang, G. Shen, K. L. Wooley, J.-S. A. Taylor, *Mol. Pharm.* **2009**, *6*, 615–626; e) M. Raouane, D. Desmaële, G. Urbinati, L. Massaad-Massade, P. Couvreur, *Bioconjugate Chem.* **2012**, *23*, 1091–1104; f) G. Maulucci et al., *Sci. Signaling* **2008**, *1*, p. l3; g) Z. Luo, K. Cai, Y. Hu, L. Zhao, P. Liu, L. Duan, W. Yang, *Angew. Chem.* **2011**, *123*, 666–669; *Angew. Chem. Int. Ed.* **2011**, *50*, 640–643; h) Y.-Z. You, Z.-Q. Yu, M.-M. Cui, C.-Y. Hong, *Angew. Chem.* **2010**, *122*, 1117–1120; *Angew. Chem. Int. Ed.* **2010**, *49*, 1099–1102; i) J. Jung, A. Solanki, K. A. Memoli, K.-i. Kamei, H. Kim, M. A. Drahl, L. J. Williams, H.-R. Tseng, K. Lee, *Angew. Chem.* **2010**, *122*, 107–111; *Angew. Chem. Int. Ed.* **2010**, *49*, 103–107.

[2] a) B. A. Kellogg et al., *Bioconjugate Chem.* **2011**, *22*, 717–727; b) C. Wu, C. Belenda, J.-C. Leroux, M. A. Gauthier, *Chem. Eur. J.* **2011**, *17*, 10064–10070; c) Y. Li, A. Nese, N. V. Lebedeva, T. Davis, K. Matyjaszewski, S. S. Sheiko, *J. Am. Chem. Soc.* **2011**, *133*, 17479–17484.

[3] a) W. Gao, R. Langer, O. C. Farokhzad, *Angew. Chem.* **2010**, *122*, 6717–6721; *Angew. Chem. Int. Ed.* **2010**, *49*, 6567–6571; b) C. D. Austin, X. Wen, L. Gazzard, C. Nelson, R. H. Scheller, S. J. Scales, *Proc. Natl. Acad. Sci. USA* **2005**, *102*, 17987–17992; c) J. Yang, H. Chen, I. R. Vlahov, J.-X. Cheng, P. S. Low, *Proc. Natl. Acad. Sci. USA* **2006**, *103*, 13872–13877; d) W. Sun, P. B. Davis, *J. Controlled Release* **2010**, *146*, 118–127; e) E. P. Feener, W. C. Shen, H. J. Ryser, *J. Biol. Chem.* **1990**, *265*, 18780–18785; f) L. R. Jones, E. A. Goun, R. Shinde, J. B. Rothbard, C. H. Contag, P. A. Wender, *J. Am. Chem. Soc.* **2006**, *128*, 6526–6527; g) Y.-J. Lee, S. Datta, J.-P. Pellois, *J. Am. Chem. Soc.* **2008**, *130*, 2398–2399; h) J. C. Cheung, P. Kim Chiaw, C. M. Deber, C. E. Bear, *J. Controlled Release* **2009**, *137*, 2–7.

[4] a) C. Lin, J. F. J. Engbersen, *J. Controlled Release* **2008**, *132*, 267–272; b) M. Breunig, C. Hozsa, U. Lungwitz, K. Watanabe, I. Umeda, H. Kato, A. Goepferich, *J. Controlled Release* **2008**, *130*, 57–63; c) M. Breunig, U. Lungwitz, R. Liebl, A. Goepferich, *Proc. Natl. Acad. Sci. USA* **2007**, *104*, 14454–14459; d) J. Li, Y. Zhu, S. T. Hazeldine, C. Li, D. Oupický, *Angew. Chem.* **2012**, *124*, 8870–8873; *Angew. Chem. Int. Ed.* **2012**, *51*, 8740–8743; e) E. Wagner, *Acc. Chem. Res.* **2011**, *45*, 1005–1013; f) D. Schaffert et al., *Angew. Chem.* **2011**, *123*, 9149–9152; *Angew. Chem. Int. Ed.* **2011**, *50*, 8986–8989; g) S. Matsumoto, R. J. Christie, N. Nishiyama, K. Miyata, A. Ishii, M. Oba, H. Koyama, Y. Yamasaki, K. Kataoka, *Biomacromolecules* **2009**, *10*, 119–127; h) M. Meyer, C. Dohmen, A. Philipp, D. Kiener, G. Maiwald, C. Scheu, M. Ogris, E. Wagner, *Mol. Pharmaceutics* **2009**, *6*, 752–762; i) S. J. Lee et al., *Angew. Chem.* **2012**, *124*, 7315–7319; *Angew. Chem. Int. Ed.* **2012**, *51*, 7203–7207; j) H. Dong, J. Lei, H. Ju, F. Zhi, H. Wang, W. Guo, Z. Zhu, F. Yan, *Angew. Chem.* **2012**, *124*, 4685–4690; *Angew. Chem. Int. Ed.* **2012**, *51*, 4607–4612; k) J.-H. Lee, K. Lee, S. H. Moon, Y. Lee, T. G. Park, J. Cheon, *Angew. Chem.* **2009**, *121*, 4238–4243; *Angew. Chem. Int. Ed.* **2009**, *48*, 4174–4179.

[5] a) N. Malik, R. Wiwattanapatapee, R. Klopsch, K. Lorenz, H. Frey, J. W. Weener, E. W. Meijer, W. Paulus, R. Duncan, *J. Controlled Release* **2000**, *65*, 133–148; b) D. Fischer, Y. Li, B. Ahlemeyer, J. Krieglstein, T. Kissel, *Biomaterials* **2003**, *24*, 1121–1131; c) Z. Kadlecova, L. Baldi, D. Hacker, F. M. Wurm, H.-A.

Klok, *Biomacromolecules* **2012**, *13*, 3127 – 3137; d) S. Aubry, F. Burlina, E. Dupont, D. Delaroche, A. Joliot, S. Lavielle, G. R. Chassaing, S. Sagan, *FASEB J.* **2009**, *23*, 2956 – 2967.
[6] S. Hong et al., *Bioconjugate Chem.* **2004**, *15*, 774 – 782.
[7] B. Wilkinson, H. F. Gilbert, *Biochim. Biophys. Acta Proteins Proteomics* **2004**, *1699*, 35 – 44.
[8] J. Koivu, R. Myllyla, T. Helaakoski, T. Pihlajaniemi, K. Tasanen, K. I. Kivirikko, *J. Biol. Chem.* **1987**, *262*, 6447 – 6449.
[9] K. Terada, P. Manchikalapudi, R. Noiva, H. O. Jauregui, R. J. Stockert, M. L. Schilsky, *J. Biol. Chem.* **1995**, *270*, 20410 – 20416.
[10] a) A. G. Torres, M. J. Gait, *Trends Biotechnol.* **2012**, *30*, 185 – 190; b) Y. Yan, Y. Wang, J. K. Heath, E. C. Nice, F. Caruso, *Adv. Mater.* **2011**, *23*, 3916 – 3921; c) B. Loretz, M. Thaler, A. Bernkop-Schnürch, *Bioconjugate Chem.* **2007**, *18*, 1028 – 1035; d) M.-H. Dufresne, M. A. Gauthier, J.-C. Leroux, *Bioconjugate Chem.* **2005**, *16*, 1027 – 1033.

